



Cite this: *Sustainable Energy Fuels*, 2024, **8**, 3329

Thermo-oxidative aging of linear and branched alcohols as stability criterion for their use as e-fuels†

Anne Lichtinger,^a Maximilian J. Poller, ^a Olaf Schröder,^b Julian Türck,^{cd} Thomas Garbe,^{eg} Jürgen Krah, ^{fg} Markus Jakob^b and Jakob Albert ^{*a}

The decarbonization of the energy supply is one of the biggest and most important challenges of the 21st century. This paper contributes to the solution of the energy crisis by investigating the stability of alcohols as e-fuels. The focus is on the investigation of the aging mechanism of the linear alcohols 1-hexanol and 1-octanol compared to the iso-alcohol 2-hexanol. It is analysed in detail how the time-dependent aging varies depending on the chain length and the position of the hydroxy-group, both in the liquid and in the gas phase. It is shown that a variety of aging products such as aldehydes, acids, short-chain alcohols and esters are formed during the aging of the *n*-alcohols by oxidation, decarboxylation, oxidative C–C bond cleavage and esterification. In contrast, the decomposition of the iso-alcohol is significantly lower. The results show that the total acid number is significantly higher for aged *n*-alcohols than for the aged iso-alcohols, while the kinematic viscosity decreases for all alcohols during aging. Carbon mass balancing shows that after accelerated aging for 120 hours, around 80% of the iso-alcohol is still present, compared to only around 57–63% for the *n*-alcohols. In addition, significantly fewer acids are formed with the iso-alcohol. In this study, iso-alcohols have a higher stability against thermo-oxidative aging compared to *n*-alcohols, showing their potential as e-fuels. Furthermore, the chain length of the alcohols has also an influence on aging, as more different aging products can be formed with increasing chain length.

Received 22nd March 2024

Accepted 17th June 2024

DOI: 10.1039/d4se00400k

rsc.li/sustainable-energy

1. Introduction

Climate change is a challenge for the world. On July 14, 2021, the EU adopted the “European Green Deal” to reduce greenhouse gas emissions by 55% until 2030 compared to 1990 levels and to achieve net zero greenhouse gas emissions by 2050.¹ Global emissions from the transport sector now account for around 25% of total greenhouse gas emissions in the EU (20% in Germany). In order to achieve climate neutrality in the EU by 2050, a 90% reduction in transport-related greenhouse gas emissions is required.¹ The war between Russia and Ukraine could have a serious impact on achieving the climate targets.²

To ensure a sustainable future, the energy sector's dependence on fossil fuels must be rapidly reduced in favour of renewable energy sources and intelligent energy solutions.² In addition to the use of electric vehicles, the use of renewable fuels such as biofuels or e-fuels, is particularly suitable for the transportation sector,^{3,4} as current political discussions show.

Alcohols, ethers and hydrocarbons are of great interest for use as e-fuels.^{5,6} As early as 1930, Fröhlich and Cryder developed a process to produce higher alcohols from synthesis gas using a Zn:Mn:Cr catalyst.^{7,8} Since then, the process has been further developed by several research groups.⁷ For example, Schemme *et al.*⁹ have developed new hydrogen-based synthetic routes for the synthesis of higher alcohols by adapting known and new chemical processes. Alcohols can also be produced from biomass, *e.g.*, through the acetone–butanol–ethanol (ABE) fermentation process.¹⁰ Sherbi *et al.*¹¹ have investigated the selective production of ring-opening products, particularly secondary alcohols, from furans and hydrogen under mild reaction conditions, thereby demonstrating a route to produce alcohols from lignocellulosic biomass using a bifunctional catalyst system consisting of platinum on a Keggin-type polyoxometalate.¹²

The use of alcohols as e-fuels can also have a positive effect on the combustion behaviour. Jakob¹³ investigated various fuels

^aHamburg University, Institute of Technical and Macromolecular Chemistry, Bundesstrasse 45, 20146, Hamburg, Germany. E-mail: jakob.albert@uni-hamburg.de

^bCoburg University of Applied Sciences and Arts, Friedrich-Streib-Strasse 2, 96450, Coburg, Germany

^cLeuphana University, Universitätsallee 1, 21335, Lueneburg, Germany

^dTECOSOL GmbH, Jahnstrasse 2, 97199, Ochsenfurt, Germany

^eVolkswagen AG, Berliner Ring 2, 38440, Wolfsburg, Germany

^fOWL University of Applied Sciences and Arts, Campusallee 12, Lemgo, 32657, Germany

^gFuels Joint Research Group, Germany; Web: <https://www.fuels-jrg.de>

† Electronic supplementary information (ESI) available. See DOI: <https://doi.org/10.1039/d4se00400k>



at an optically accessible single-cylinder diesel engine at a defined part-load operation point with fuel individual EGR rates for 100 ppm NO_x raw emissions and fuel individual starts of the single main injection for fixed center of combustion. The results show that oxygenated molecules provide the potential for decreased in-cylinder soot formation in comparison to EN590 diesel. The decreased in-cylinder soot formation tendency with similar NO_x raw emissions results in decreased particle raw emissions with marginal drawbacks in CO and HC raw emissions. Nour *et al.*¹⁴ carried out combustion tests in a DI diesel engine with blends of 1-hexanol and diesel of 10–50%. They found that a reduction in NO_x and smoke can be achieved without compromising performance by using 1-hexanol diesel blends compared to the use of pure diesel. Garcia *et al.*¹⁵ carried out performance and engine exhaust measurements on a single-cylinder engine at four different engine operating conditions of 1-octanol, di-*n*-butyl ether and various blends. They found, that all used fuels show a considerable reduction in soot emissions with the same NO_x values. In addition, the used alternative fuels improve fuel conversion in terms of efficiency.

If a fuel is stored for a longer period of time, for example to build up a supply as a kind of “chemical battery” during the current war, fuel aging can occur. This is defined as the change in chemical and physical properties over time.³ These changes can result in colour change, change in fuel composition, combustion properties and compatibility with other fuels.^{16,17} In addition to microbiological aging, oxidation is the most important chemical reaction that triggers fuel aging.³ Both fossil diesel fuel and gasoline can age due to autoxidation.^{16–19} If metals are present in the fuel, the oxidation rate can increase.¹⁸ During aging, the olefins and diolefins in the fuel are oxidized first, which increases the oxygen content in the fuel.^{16,18} In the case of gasoline, the volatile components can evaporate during aging.^{16,17} Both gasoline and diesel show a decrease in aromatics in the fuel and resin-like precipitate formation, therefore “gum formation” can occur.^{16–19} The formed precipitate consists of highly aromatic compounds with a molecular weight of 200–500 Da, as well as cyclic and branched olefins. Esters, carboxylic acids and ethers can also be contained in the gum.^{16,18} The gum can lead to deposits on the fuel filter and blockage of engine parts.¹⁹ It can also affect the combustion of the fuel, which can lead to a change in engine performance and increased CO and NO_x emissions.^{16,17} If the fossil fuel is mixed with alcohol, aging shows that the alcohol does not act as a catalyst or inhibitor for autoxidation. In addition, the deposition of precipitates is reduced because the alcohols which are more polar than diesel or gasoline keep the polar precipitates in solution.¹⁷ Aging also occurs in biodiesel due to autoxidation.^{20–23} Aldehydes, ketones and carboxylic acids can be formed.²⁴ However, oligomers can also be formed,^{25,26} which can lead to clogging of the fuel filter.²⁷ The aging of conventional fuels is well studied, while research into the aging of e-fuels is still in its infancy. However, studies on the aging of e-fuels are an important prerequisite for the approval and use of e-fuels.

The detailed investigation of the aging mechanism of alcohols as e-fuels has only been little studied in literature. Several

research groups have investigated the oxidation of primary alcohols with the aid of catalysts for synthesis purposes (to increase yield and product selectivity).^{28–36} For example, Ishida *et al.*³⁰ Kotolevich *et al.*,³² Jenzer *et al.*³⁴ and Iwahama *et al.*³⁵ oxidized 1-octanol using various catalysts and found several aging products (aldehydes, acids, esters). Hussein *et al.*³¹ also found an ether and a peroxy-acetal as aging products. Guillard *et al.*³⁶ oxidized 1-octanol with ultrasound and photocatalysis and detected several aldehydes, alkanes and alkenes as aging products. Gallot *et al.*²⁹ investigated the oxidation of 2-hexanol to a ketone using a catalyst whereby Mosher and Preiss³³ studied the acid-catalysed oxidation of various alcohols, *e.g.*, 2-pentanol and 2-methyl-1-propanol. They found aldehydes, acetals, hemiacetals and esters as decomposition products.³³

In this paper, the time-dependent, thermo-oxidative aging of various alcohols with different chain length and position of the hydroxy-group is investigated, both in the liquid and in the gas phase. The carbon mass balance of the aged products and the investigation of important fuel-specific parameters (total acid number, kinematic viscosity) allow for a detailed elucidation of the aging mechanism.

2. Materials and methods

2.1. Fuels and chemicals

1-hexanol with a purity > 98%, 1-octanol with a purity > 99%, tetrahydrofuran, and the 30% aqueous hydrogen peroxide solution were purchased from Carl Roth. 2-Hexanol with a purity > 98% was purchased from Alfa Aesar. The chemicals for calibration for concentration determination were purchased from Alfa Aesar and Sigma Aldrich. All chemicals were used as received without further purification.

2.2. Experimental setup and work procedure of fuel aging

2.2.1. Open aging setup for accelerated aging (setup 1). For accelerated thermo-oxidative aging the aging setup which is described in a previous article³ was used. It consists of a 250 mL three-neck round bottom flask, which was filled with 250 mL (at the start of aging) of the fuel to be aged (Fig. 1, I). The flask was then placed in the oil bath (Fig. 1, II), which was heated using

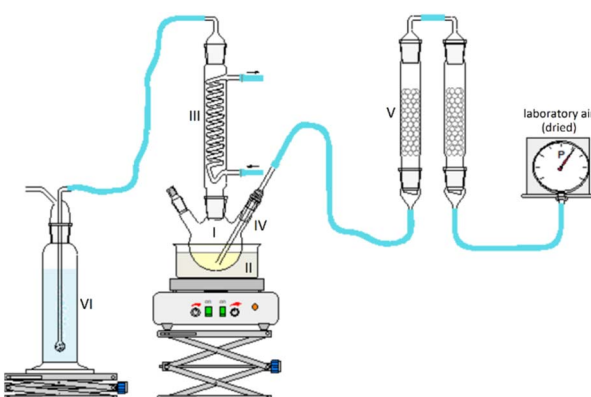


Fig. 1 Open aging setup for accelerated laboratory aging (setup 1).



a heating plate to maintain a temperature of $T = 110\text{ }^{\circ}\text{C}$. In order to minimize the release of volatile aging products, a Dimroth reflux condenser (Fig. 1, III) was positioned above the flask and maintained at a constant temperature of $T = 2\text{ }^{\circ}\text{C}$ using a recirculating chiller (F series from Julabo). Condensation was observed only in the lower section of the reflux condenser during the aging process. To oxidize the fuel, dry compressed air, which was additionally dehumidified using a molecular sieve (4 Å) (Fig. 1, V), was introduced into the fuel at a constant flow rate of 10 L h^{-1} via a gas introduction tube connected to the three-neck flask (Fig. 1, IV). The air flow rate was regulated using an Agilent Flow Tracker 1000 flowmeter. This aging setup operated as an open aging system. The air introduced into the fuel was directed through the reflux condenser and a wash bottle containing deionized water (Fig. 1, VI). To initiate the fuel aging process, the reflux condenser and oil bath were preheated to the desired temperature, and the air flow rate was adjusted accordingly. The gas introduction tube and the reflux condenser were then connected to the three-neck flask filled with 250 mL of fuel, and the flask was immersed in the temperature-controlled oil bath. This marked the start of the experiment ($t = 0\text{ h}$). To monitor the aging products over time, a 25 mL fuel sample was withdrawn from the flask every 24 hours. The stopper on the flask was briefly opened, and a glass pipette was used to extract 25 mL of the aged fuel. This sampling procedure was repeated until a total aging time of 192 hours was reached. Afterwards, the air flow and heating plate for the oil bath were turned off. The remaining fuel, along with any condensate present in the reflux condenser, was collected after a cooling phase. Both the unaged fuel (0 h) and the aged fuel samples (24–192 h) were subjected to subsequent analysis.

2.2.2. Closed aging setup for accelerated aging (setup 2). In order to perform carbon mass balancing of the aged fuels, both the liquid phase and the gas phase of the aged fuels must be examined. For this purpose, a closed aging setup was developed. 50 mL of the fuel to be aged is contained in a 100 mL two-neck flask (cf. Fig. 2, I). The two-neck flask was placed in an oil

bath (cf. Fig. 2, II), which was tempered to $T = 120\text{ }^{\circ}\text{C}$ using a magnetic stirring and heating plate. On top of the two-neck flask a Dimroth reflux condenser (cf. Fig. 2, III) was placed, which was cooled to $T = 2\text{ }^{\circ}\text{C}$ with the aid of a recirculating condenser to prevent evaporation of readily volatile aging products. The gas phase of the aged fuel that nevertheless arose was collected by a gas bag (cf. Fig. 2, IV) attached to the upper end of the reflux condenser by means of a hose. The other opening of the two-necked flask was closed with a septum (cf. Fig. 2, V) to ensure the system was completely sealed. This was checked prior to the start of aging using a soap solution and gas flowed in. As oxidant, 20 mL of a 30% aqueous hydrogen peroxide solution was used for this aging. To ensure mixing of the fuel with the oxidant, a magnetic stirrer was located in the two-neck flask by which the fuel was continuously stirred. Prior to aging, the complete system was purged with an inert gas (nitrogen) to ensure that any gaseous products detected in the gas bag were the result of aging only. At the beginning of aging ($t = 0\text{ h}$), the first 8 mL of the hydrogen peroxide solution was introduced into the fuel through the septum (cf. Fig. 2, V) using a syringe. After 24 h of aging, another 8 mL of the hydrogen peroxide solution was added to the fuel through the septum, and after another 24 h (48 h of aging), the remaining 4 mL of the hydrogen peroxide solution was added. After 120 h of aging (end of aging), the liquid phase of the aged fuel (in the two-neck flask) and the gaseous phase of the aged fuel (in the gas bag) were analysed after cooling to ambient temperature.

2.3. Analytical methods

2.3.1. Gas chromatography with coupled mass spectrometry (GC-MS). For the GC-MS measurements, an Agilent GC7890A gas chromatograph coupled with an Agilent 5973 quadrupole mass spectrometer was employed. The GC-MS system utilized a Phenomenex Zebron ZB-5 HT column with a length of 30 m, an inner diameter of 0.25 mm, and a film thickness of 0.25 μm . Helium served as the carrier gas at a flow rate of 49.8 mL min^{-1} . In the temperature program, the furnace was first held at $40\text{ }^{\circ}\text{C}$ for 15 min and then brought to $100\text{ }^{\circ}\text{C}$ at $3\text{ }^{\circ}\text{C min}^{-1}$. After holding for 15 min, the oven was brought to $180\text{ }^{\circ}\text{C}$ at $5\text{ }^{\circ}\text{C min}^{-1}$ and then to $250\text{ }^{\circ}\text{C}$ at $10\text{ }^{\circ}\text{C}$. $2\text{ }\mu\text{L}$ were injected and the split ratio was 60 : 1. For analysis, $10\text{ }\mu\text{L}$ of the sample was mixed with $5\text{ }\mu\text{L}$ of tetrahydrofuran as an internal standard and 1 mL of acetonitrile and used as a sample for GC-MS analysis. For product identification, the spectra were compared to the NIST08 database. To determine the concentration of the aging products, a calibration series was performed with each of the pure substances together with the internal standard tetrahydrofuran. For the aging products that could not be obtained in pure form, instead of determining the concentration, the peaks of the products were integrated and the areas of the products were divided by the peak areas of the internal standard (peak area_{analyte}/peak area_{internalstandard}).

2.3.2. Gas chromatography with a thermal conductivity detector (GC-TCD). Quantification of the gaseous phase was accomplished utilizing a Varian GC 450-TCD with a Shin Carbon ST column (2 m \times 0.75 mm). The gaseous sample was

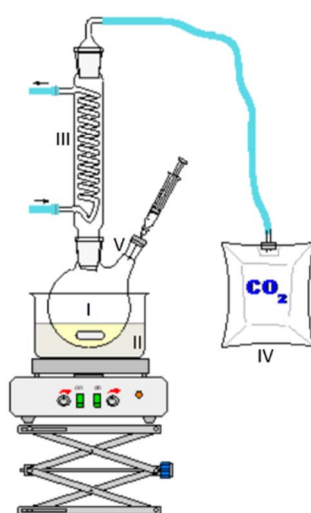


Fig. 2 Closed aging setup for accelerated laboratory aging (setup 2).



collected in a gas bag and injected using argon as mobile phase at a pressure of 4.82 bar. The following temperature program was used: 40 °C (1.5 min), 18 °C min⁻¹ to 250 °C, 250 °C (12 min).

2.3.3. Total acid number (TAN). The determination of the total acid number for both the unaged and aged fuels followed the potentiometric titration method according to DIN EN 12634. To conduct these measurements, an 888 Titrando and an 801 stirrer, both from Metrohm, were employed. A glass electrode suitable for non-aqueous media was used for the titration process. The measuring solution consisted of a potassium hydroxide solution (0.1 mol L⁻¹) dissolved in 2-propanol. The solvent utilized in the analysis was composed of 50% toluene, 49.5% 2-propanol, and 0.5% deionized water, with a volume of 60 mL per sample. The sample weight varied depending on the expected total acid number, ranging from 0.505 g to 10.007 g. The total acid number represents the quantity of base, expressed in milligrams of potassium hydroxide per gram fuel (mg KOH per g), necessary to neutralize the acids present in the sample.

2.3.4. Kinematic viscosity. The kinematic viscosity of the unaged and aged fuels was assessed using a Stabinger viscosimeter from Anton Paar. To conduct the measurements, a syringe was utilized to inject 3 mL of the sample into the instrument. The viscosity measurements were carried out at a temperature of 40 °C. Data processing of the measurements was performed using Anton Paar's Rheoplus software.

2.3.5. Carbon mass balancing. In order to close the carbon mass balance of the aged products, the alcohols were aged in the closed aging system (setup 2, *cf.* Section 2.2.2). The volume of the gas phase was determined by the buoyancy method (Archimedes' principle) and the mass of the products in the gas phase could be calculated *via* the concentration of the detected products in the gas phase. When the alcohols were aged with a hydrogen peroxide solution, an organic and an aqueous liquid phase were formed. The two phases were separated with the aid

of a separating funnel and the volume of the organic and aqueous phases was determined with a graduated cylinder. By determining the concentration of the products in the organic and in the aqueous phase, the total mass of the products in the liquid phase could be determined to get the carbon mass balance.

3. Results and discussion

3.1. Qualitative analysis of thermo-oxidative aging

In order to determine which kind of products are formed during aging, the alcohols 1-hexanol, 1-octanol, and 2-hexanol were aged for up to 192 h using the open aging setup (setup 1, *cf.* Section 2.2.1). The aging products detected by GC-MS (*cf.* Section 2.3.1) and the corresponding aging times at which they were detected are listed in Table 1.

3.1.1. Qualitative analysis of the aging of 1-hexanol and 1-octanol. To explain the decomposition of 1-hexanol by thermo-oxidative aging, the reaction pathways shown in Fig. 3 were revealed. All products detected by GC-MS are highlighted. However, some intermediates are either volatile or quickly react further, so that not all postulated aging products (*cf.* Fig. 3) could be found by GC-MS. However, in order to explain the formation of the products found in the GC-MS in a meaningful way, the following aging pathways (Fig. 3–5) are suggested.

After 24 hours, 1-hexanal was detected as a first aging product resulting from the oxidation of 1-hexanol. The oxidation may take place *via* the reaction mechanism proposed by Li.³⁷ Alternatively, the aldehyde could also be formed *via* autoxidation of the *n*-alcohol.^{38,39} After 48 h aging time, hexanoic acid could also be detected. Hexanal could be further oxidized to hexanoic acid by autoxidation^{39,40} of the aldehyde to a percarboxylic acid and subsequent conversion of the percarboxylic acid to a carboxylic acid.^{41,42} Also, the two esters hexyl hexanoate and hexyl formate as well as the *n*-alcohol 1-pentanol have been detected after 48 h. The resulting hexanoic acid can

Table 1 Aging products (GC-MS) of the aging of 1-hexanol, 1-octanol, and 2-hexanol

1-Hexanol (aging products)	1-Octanol (aging products)	2-Hexanol (aging products)
1-Hexanol (0–192 h)	1-Octanol (0–192 h)	2-Hexanol (0–192 h)
Hexanal (24–192 h)	1-Heptanol (24–192 h)	2-Hexanone (48–192 h)
1-Pentanol (48–192 h)	Octanal (24–192 h)	1-Butanol (96–192 h)
Hexanoic acid (48–192 h)	Octanoic acid (24–192 h)	Acetic acid (96–192 h)
Hexyl formate (48–192 h)	Octyl formate (24–192 h)	2-Hexyl acetate (96–192 h)
Hexyl hexanoate (48–192 h)	Octyl octanoate (24–192 h)	2-Hexyl formate (120–192 h)
1-Butanol (72–192 h)	Heptanal (48–192 h)	Butanoic acid (168–192 h)
Pentanal (72–192 h)	1-Hexanol (72–192 h)	
Pentanoic acid (72–192 h)	Heptanoic acid (72–192 h)	
Hexyl acetate (72–192 h)	Octyl acetate (72–192 h)	
Hexyl pentanoate (72–192 h)	Octyl heptanoate (72–192 h)	
Butanoic acid (96–192 h)	1-Pentanol (96–192 h)	
Hexyl butanoate (96–192 h)	Hexanoic acid (96–192 h)	
Hexyl propanoate (120–192 h)	Octyl propanoate (96–192 h)	
	Octyl hexanoate (96–192 h)	
	1-Butanol (120–192 h)	
	Pentanoic acid (120–192 h)	
	Octyl butanoate (120–192 h)	
	Octyl pentanoate (120–192 h)	



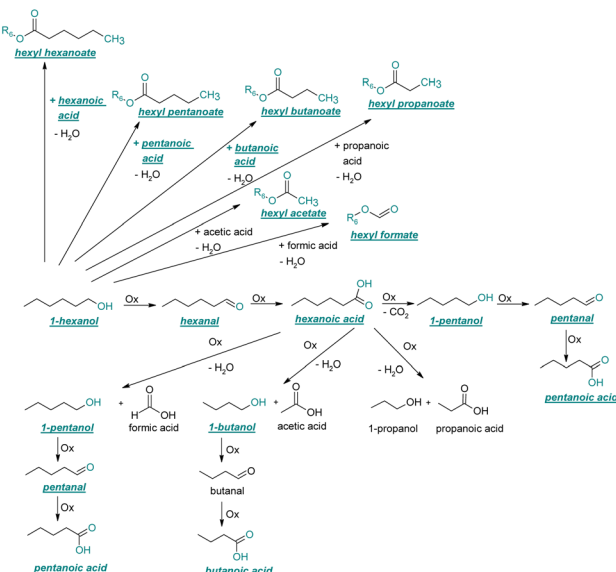


Fig. 3 Reaction pathway of the thermo-oxidative aging of 1-hexanol. Directly observed compounds are highlighted.

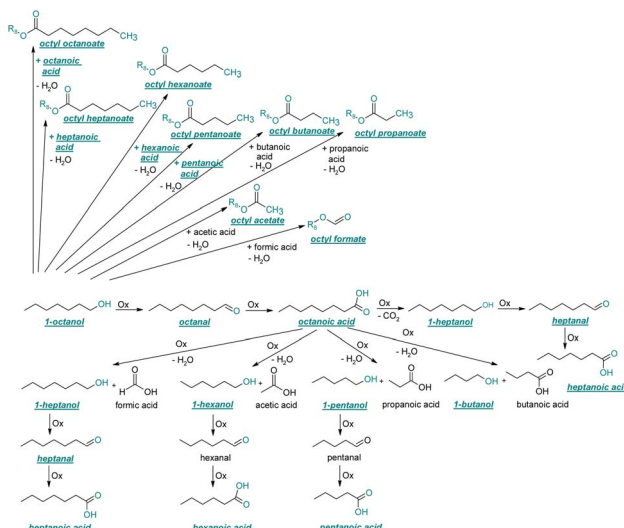


Fig. 4 Reaction pathways of the thermo-oxidative aging of 1-octanol. Directly observed compounds are highlighted.

be esterified with the existing alcohol 1-hexanol to form the ester hexyl hexanoate. A possibility for the formation of 1-pentanol is an oxidative decarboxylation of hexanoic acid with CO_2 as by-product. Another explanation for the formation of 1-pentanol could be an oxidative C-C bond cleavage of hexanoic acid into shorter-chain alcohols and carboxylic acids. Depending on the position of the C-atom at which the bond cleavage occurs, several carboxylic acids and *n*-alcohols can be formed. Table 2 gives an overview of the carboxylic acids and *n*-alcohols formed in this way. The starting products for the oxidative C-C bond cleavage are hexanoic acid and octanoic acid. The second product that can be formed in addition to 1-pentanol by oxidative C-C bond cleavage of hexanoic acid is formic acid (*cf.*

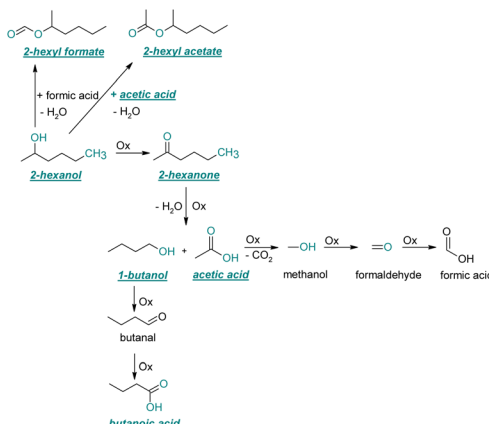


Fig. 5 Reaction pathways of the thermo-oxidative aging of 2-hexanol. Directly observed compounds are highlighted.

Table 2 Aging products of the oxidative C-C bond cleavage depending on the position of the C-atom

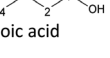
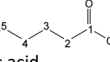
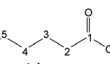
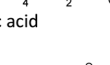
Intermediate	Position	Products
 hexanoic acid	2	$\text{CCCCCCOH} + \text{O}=\text{O} + \text{H}_2\text{O}$ 1-pentanol+formic acid $+ \text{H}_2\text{O}$
 hexanoic acid	3	$\text{CCCCCOH} + \text{C}(=\text{O})\text{OH} + \text{H}_2\text{O}$ 1-butanol+acetic acid $+ \text{H}_2\text{O}$
 hexanoic acid	4	$\text{CCCCCOH} + \text{CH}_3\text{CH}_2\text{CH}_2\text{OH} + \text{H}_2\text{O}$ 1-propanol+propanoic acid $+ \text{H}_2\text{O}$
 octanoic acid	2	$\text{CCCCCCCCOH} + \text{O}=\text{O} + \text{H}_2\text{O}$ 1-heptanol+formic acid $+ \text{H}_2\text{O}$
 octanoic acid	3	$\text{CCCCCCCCOH} + \text{C}(=\text{O})\text{OH} + \text{H}_2\text{O}$ 1-hexanol+acetic acid $+ \text{H}_2\text{O}$
 octanoic acid	4	$\text{CCCCCCCCOH} + \text{CH}_3\text{CH}_2\text{CH}_2\text{OH} + \text{H}_2\text{O}$ 1-pentanol+propanoic acid $+ \text{H}_2\text{O}$
 octanoic acid	5	$\text{CCCCCCCCOH} + \text{CH}_3\text{CH}_2\text{CH}_2\text{CH}_2\text{OH} + \text{H}_2\text{O}$ 1-butanol+butanoic acid $+ \text{H}_2\text{O}$
 2-hexanone	3	$\text{CCCCCOH} + \text{C}(=\text{O})\text{OH} + \text{H}_2\text{O}$ 1-butanol+acetic acid $+ \text{H}_2\text{O}$

Table 2). The latter can be esterified with 1-hexanol to form hexyl formate. After 72 h aging time pentanal, pentanoic acid, 1-butanol, hexyl acetate and hexyl pentanoate have been detected. 1-Pentanol could be oxidized to pentanal and further oxidized to pentanoic acid.³⁸⁻⁴¹ The latter can then be esterified with 1-hexanol to hexyl pentanoate. An explanation for the formation

of 1-butanol and hexyl acetate could be the oxidative C–C bond cleavage of hexanoic acid (*cf.* Table 2) to acetic acid and 1-butanol and the esterification of 1-hexanol and acetic acid to hexyl acetate. The analysis of the aging products after 96 h aging time showed the formation of butanoic acid and hexyl butanoate. The resulting 1-butanol could be oxidized to butanal and further oxidized to butanoic acid. The latter can then be esterified with 1-hexanol to hexyl butanoate. After 120 h aging time, hexyl propanoate has been detected. An explanation could be the oxidative C–C bond cleavage of hexanoic acid to 1-propanol and propanoic acid (*cf.* Table 2) and the esterification of 1-hexanol and propanoic acid to hexyl propanoate. The GC-MS analysis showed, that all detected aging products that have been formed until 120 h, could also be detected after 144 h, 168 h, and 192 h aging time, respectively (*cf.* Table 1).

The thermo-oxidative aging of the *n*-alcohol 1-octanol produces more products than the aging of 1-hexanol. Fig. 4 shows the proposed reaction pathway. All products detected by GC-MS are highlighted. After 24 h aging time octanal, octanoic acid, 1-heptanol, octyl formate, and octyl octanoate have been detected. 1-Octanol could be first oxidized to octanal and further to octanoic acid.^{38–40} The latter can be esterified with 1-octanol to form octyl octanoate. The octanoic acid could also be cleaved into 1-heptanol and formic acid by oxidative C–C bond cleavage (*cf.* Table 2) and the esterification of 1-octanol and formic acid forms octyl formate. After 48 h aging time 1-heptanal has been detected resulting from 1-heptanol oxidation.^{37–39} After 72 h the GC-MS analysis showed the formation of heptanoic acid, 1-hexanol as well as octyl acetate and octyl heptanoate. The formation of heptanoic acid can be explained by the oxidation of heptanal^{39,40} and the esterification of heptanoic acid and 1-octanol forms octyl heptanoate. The oxidative C–C bond cleavage of octanoic acid to 1-hexanol and acetic acid (*cf.* Table 2) and the subsequent esterification of acetic acid and 1-octanol to octyl acetate is a possible explanation for the formation of the other detected aging products after 72 h. After 96 h thermo-oxidative aging, hexanoic acid, 1-pentanol, octyl propanoate, and octyl hexanoate have also been detected. The formed 1-hexanol could be oxidized to hexanal and further oxidized to hexanoic acid and 1-octanol, whereas hexanoic acid can be esterified to octyl hexanoate. An explanation for the formation of 1-pentanol and octyl propanoate could be the oxidative C–C bond cleavage of octanoic acid to 1-pentanol and propanoic acid (*cf.* Table 2) and further esterification of 1-octanol and propanoic acid to octyl propanoate. After 120 h aging time, GC-MS analysis showed pentanoic acid, 1-butanol, octyl butanoate, and octyl pentanoate formation. The formed 1-pentanol could be oxidized to pentanal and further to pentanoic acid. 1-octanol and pentanoic acid can be esterified to octyl pentanoate. The oxidative C–C bond cleavage of octanoic acid could lead to 1-butanol and butanoic acid (*cf.* Table 2) and the esterification of 1-octanol and butanoic acid forms octyl butanoate. All detected aging products that have been formed until 120 h, could also be detected after 144 h, 168 h, and 192 h aging time (*cf.* Table 1).

3.1.2. Qualitative analysis of the aging of 2-hexanol. The aging of the iso-alcohol 2-hexanol produces fewer aging

products than the corresponding *n*-alcohol 1-hexanol (*cf.* Table 1). Fig. 5 shows the proposed reaction mechanism for the aging of 2-hexanol. The products detected by GC-MS are highlighted.

After 48 h aging time 2-hexanone was detected as an aging product. An explanation for its formation is the oxidation of 2-hexanol to 2-hexanone. The reaction mechanism proposed by Li³⁷ could possibly come into play here. Alternatively, the ketone could also be formed from the iso-alcohol by autoxidation.^{38,39} After 96 h aging time, 1-butanol, acetic acid, and the ester 2-hexyl acetate were also detected as aging products. These are formed due to an oxidative C–C bond cleavage of 2-hexanone to 1-butanol and acetic acid (*cf.* Table 2). Acetic acid can then be esterified with 2-hexanol to 2-hexyl acetate. After 120 h aging time, 2-hexyl formate was detected as an additional aging product. An explanation for this could be an oxidative decarboxylation of acetic acid to methanol with CO₂ as by-product, and an oxidation of methanol to formaldehyde and further oxidation to formic acid.^{38–40,42} An esterification of 2-hexanol and formic acid can form 2-hexyl formate. After 168 h aging time butanoic acid was detected as aging product. The formed 1-butanol can be oxidized to butanal and further oxidized to butanoic acid.^{38–40,42} All detected aging products that have been formed until 168 h could also be detected after 192 h aging time (*cf.* Table 1).

3.2. Quantitative analysis of thermo-oxidative aging

As the composition of fuels can change during aging, it is important to further quantify the aging products. In order to quantitatively analyse the aging products formed during aging, the concentration of the products is considered as a function of the aging time. For this purpose, the samples from the above-described experiment were investigated quantitatively using GC-MS.

3.2.1. Quantitative analysis of the aging of 1-hexanol.

Fig. 6a and b show the concentration of various aging products of 1-hexanol as a function of aging time and Fig. 6c shows the peak area normalized by the internal standard as a function of aging time. After 24 h aging time, hexanal is formed with a concentration of $c = 0.064 \text{ mg mL}^{-1}$. At the same time, the concentration of 1-hexanol decreases by ~8% from $c = 8.14 \text{ mg mL}^{-1}$ to $c = 7.48 \text{ mg mL}^{-1}$. From an aging time of 48 h, hexanoic acid is formed with a concentration of $c = 0.156 \text{ mg mL}^{-1}$. Furthermore, the two esters hexyl hexanoate with a concentration of $c = 0.0038 \text{ mg mL}^{-1}$ and hexyl formate with $c = 0.028 \text{ mg mL}^{-1}$, as well as 1-pentanol with a concentration of $c = 0.054 \text{ mg mL}^{-1}$ are formed. Compared to the concentration at 24 h, the concentration of 1-hexanol decreases by a further 8% to a value of $c = 6.85 \text{ mg mL}^{-1}$, while the concentration of hexanal continues to increase to a value of $c = 0.068 \text{ mg mL}^{-1}$. From 72 h aging time, pentanal and pentanoic acid as well as 1-butanol and the two esters hexyl acetate ($c = 0.0061 \text{ mg mL}^{-1}$) and hexyl pentanoate are formed (*cf.* Fig. 6b and c). From 96 h the ester hexyl butanoate ($c = 0.014 \text{ mg mL}^{-1}$) is formed and from ~120 h the ester hexyl propanoate ($c = 0.0034 \text{ mg mL}^{-1}$) is formed (*cf.* Fig. 6b).

Considering the progression of the concentration or the normalized peak area of the aging products over time (*cf.*



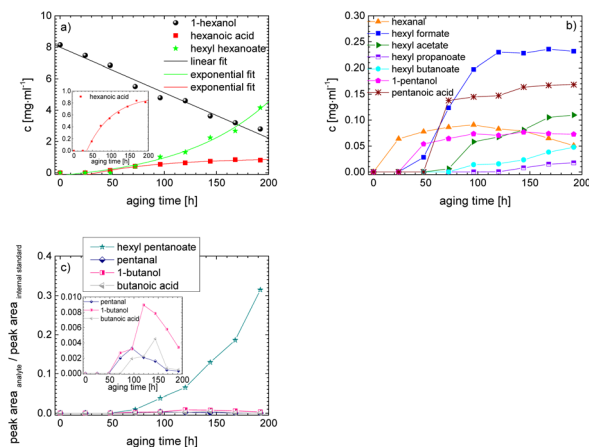


Fig. 6 (a and b) Concentration as a function of the aging time of various decomposition products of the thermo-oxidative aging of 1-hexanol. (c) Normalized peak area as a function of the aging time of various products of the thermo-oxidative aging of 1-hexanol.

Fig. 6a–c), it can be observed that the concentration of 1-hexanol steadily decreases to ~65% of the initial concentration after 192 h aging time. This is due to the formation of various aldehydes, acids, and esters. The concentration of hexanal initially increases from 24 h to 96 h, reaches a maximum value of $c = 0.091 \text{ mg mL}^{-1}$ at 96 h, and then decreases again to $c = 0.051 \text{ mg mL}^{-1}$ at 192 h. This is possibly due to the fact that hexanal is continuously formed by oxidation of 1-hexanol, but is then further oxidized to hexanoic acid. The formed hexanoic acid increases from 48 h to $c = 0.840 \text{ mg mL}^{-1}$ at 168 h and then decreases to $c = 0.815 \text{ mg mL}^{-1}$ at 192 h. The renewed decrease can be possibly explained by the fact that although hexanal is continuously oxidized to hexanoic acid, the hexanoic acid is further esterified to hexyl hexanoate and can also be cleaved to shorter-chain acids and *n*-alcohols by oxidative C–C bond cleavage. The pentanoic acid formed from 72 h increases steadily up to 192 h to $c = 0.168 \text{ mg mL}^{-1}$. An explanation for the steady increase could be that pentanoic acid can be formed from hexanoic acid both by oxidative C–C bond cleavage and by oxidative decarboxylation and subsequent oxidation. 1-Pentanol increases slightly from 48 h to 192 h up to a value of $c = 0.073 \text{ mg mL}^{-1}$. The ester hexyl hexanoate increases steadily from 48 h up to a value of $c = 4.17 \text{ mg mL}^{-1}$ at 192 h. The other formed esters (hexyl formate, hexyl acetate, hexyl propanoate and hexyl butanoate) increase steadily at the beginning, but then reach a plateau after a certain time. This can be possibly explained by the fact that hexyl hexanoate can be esterified directly from 1-hexanol and hexanoic acid, whereas for the other esters the corresponding acids must first be formed from hexanoic acid. The direct esterification of hexyl hexanoate is much more likely. This is also shown by the maximum concentration at 192 h of the formed esters:

$$\begin{aligned} c_{\text{hexylhexanoate}} &= 4.17 \text{ mg mL}^{-1} \gg c_{\text{hexylformate}} = 0.232 \text{ mg mL}^{-1} \\ c_{\text{hexylacetate}} &= 0.110 \text{ mg mL}^{-1} > c_{\text{hexylbutanoate}} = 0.0475 \text{ mg mL}^{-1} \\ c_{\text{hexylpropanoate}} &= 0.0174 \text{ mg mL}^{-1} \end{aligned}$$

Considering the progression of the normalized peak area of hexyl pentanoate over time, it can be seen that hexyl pentanoate increases steadily up to 192 h and does not show a plateau. This can be possibly explained by the fact that 1-pentanol, which can be further oxidized to pentanoic acid, can be formed both by oxidative decarboxylation and by oxidative C–C bond cleavage (cf. Fig. 3 and 6a–c).

3.2.2. Quantitative analysis of the aging of 1-octanol.

Fig. 7a–c show the concentration profiles resp. The peak area normalized by the internal standard as a function of the aging time of the decomposition products of the thermo-oxidative aging of 1-octanol. From 24 h aging time, the initial concentration of 1-octanol decreases by 7% from $c = 8.03 \text{ mg mL}^{-1}$ to $c = 7.47 \text{ mg mL}^{-1}$. At the same time, both the aldehyde octanal ($c = 0.153 \text{ mg mL}^{-1}$) and octanoic acid ($c = 0.010 \text{ mg mL}^{-1}$) are formed (cf. Fig. 7a and b). Due to the presence of octanoic acid, the two esters octyl octanoate ($c = 0.00123 \text{ mg mL}^{-1}$) and octyl formate ($c = 0.0183 \text{ mg mL}^{-1}$) as well as 1-heptanol ($c = 0.00324 \text{ mg mL}^{-1}$) are formed from 24 h onwards. Heptanal is formed from 48 h (cf. Fig. 7c). From 72 h, heptanoic acid ($c = 0.00769 \text{ mg mL}^{-1}$) and octyl heptanoate are formed. Furthermore, 1-octanol ($c = 0.00127 \text{ mg mL}^{-1}$) and the ester octyl acetate ($c = 0.00599 \text{ mg mL}^{-1}$) are formed. From an aging time of 96 h, hexanoic acid, 1-pentanol ($c = 0.00599 \text{ mg mL}^{-1}$) and the two esters octyl propanoate and octyl hexanoate are formed (cf. Fig. 7b and c). From 120 h, the two esters octyl butanoate ($c = 0.00446 \text{ mg mL}^{-1}$) and octyl pentanoate are formed (cf. Fig. 7b and c). After 192 h of aging, the initial concentration of 1-octanol (cf. Fig. 7a) decreases by ~73%, in contrast to the aging of 1-hexanol (cf. Fig. 6 a), where the initial concentration only decreases by ~65% after 192 h. The decrease is possibly due to the fact that 1-octanol reacts by oxidation and esterification to form various aldehydes, acids, and esters. The concentration of octanal shows a maximum at 24 h ($c = 0.153 \text{ mg mL}^{-1}$) and then decreases steadily until it reaches a value of $c = 0.0298 \text{ mg mL}^{-1}$ at 192 h (cf. Fig. 7b). This shows a difference to the thermo-oxidative aging of 1-hexanol. 1-Hexanal shows its maximum concentration not at 24 h, but at 96 h (cf. Fig. 6b). Octanoic acid increases continuously from 24 h to 192 h, up to a value of $c = 0.939 \text{ mg mL}^{-1}$ (cf. Fig. 7a). This represents a further difference to the aging of 1-hexanol, because the formed hexanoic acid at the aging of 1-hexanol shows a maximum concentration at 168 h, after which its concentration decreases again (cf. Fig. 6a). The two resulting *n*-alcohols 1-heptanol and 1-octanol show a maximum at 144 h, while heptanoic acid shows a maximum at 168 h (cf. Fig. 7b). The ester octyl formate increases continuously up to a value of $c = 0.410 \text{ mg mL}^{-1}$ at 192 h and then shows a plateau (cf. Fig. 7b). The other formed esters increase continuously up to 192 h (cf. Fig. 7b and c), while the esters formed during 1-hexanol aging (with the exception of hexyl hexanoate) all show a plateau (cf. Fig. 7a–c). The concentration of octyl octanoate after 192 h is significantly higher than the concentration of the other esters, $c_{\text{octyloctanoate}} = 2.89 \text{ mg mL}^{-1} \gg c_{\text{octylformate}} = 0.410 \text{ mg mL}^{-1} > c_{\text{octylacetate}} = 0.0756 \text{ mg mL}^{-1} > c_{\text{octylbutanoate}} = 0.0571 \text{ mg mL}^{-1}$. This is possibly due to the fact that octyl octanoate can be esterified directly from the

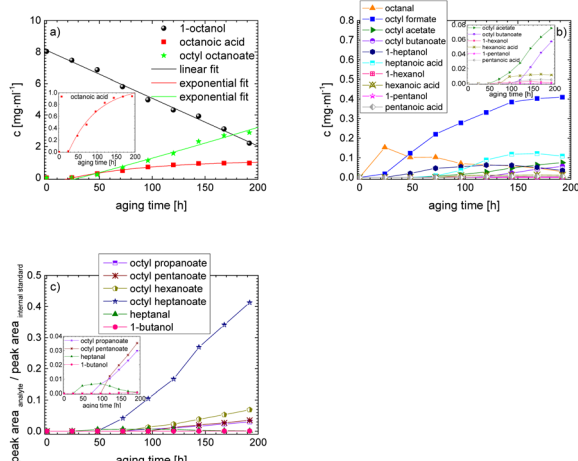


Fig. 7 (a and b) Concentration as a function of the aging time of various products of the thermo-oxidative aging of 1-octanol. (c) Normalized peak area as a function of the aging time of various products of the thermo-oxidative aging of 1-octanol.

resulting octanoic acid, whereas formic, acetic or butyric acid must first be formed from octanoic acid by oxidative C-C bond cleavage, which is less likely. The results show that 1-octanol is less stable against thermo-oxidative aging than 1-hexanol. This can be seen, among other things, from the fact that more aging products are formed during the aging of 1-octanol (*cf.* Fig. 4 and Table 1). The chain length of the *n*-alcohols therefore appears to have an influence on aging.

3.2.3. Quantitative analysis of the aging of 2-hexanol. The thermo-oxidative aging of the C₆-iso-alcohol 2-hexanol produces fewer aging products than the C₆-*n*-alcohol 1-hexanol or the C₈-*n*-alcohol 1-octanol. Fig. 8a and b show the concentration resp. the peak area normalized by the internal standard as a function of the aging time of the decomposition products of 2-hexanol. From an aging time of 48 h, the ketone 2-hexanone is formed with a concentration of $c = 0.515 \text{ mg mL}^{-1}$. The concentration of 2-hexanone increases at 72 h to $c = 1.11 \text{ mg mL}^{-1}$ (cf. Fig. 8a), while the initial concentration of 2-hexanol decreases by $\sim 21\%$ to $c = 6.88 \text{ mg mL}^{-1}$. From an aging time of ~ 96 h, acetic acid is formed with a concentration of $c = 0.00150 \text{ mg mL}^{-1}$ as well as 1-butanol and 2-hexyl acetate (cf. Fig. 8a and b). From 120 h the ester 2-hexyl formate is formed, and from 168 h butyric acid is formed (cf. Fig. 8b). Up to an aging time of 192 h, the initial

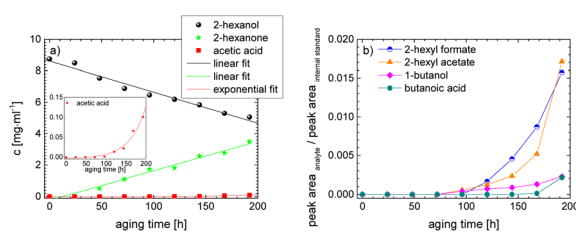


Fig. 8 (a) Concentration as a function of the aging time of various products of the thermo-oxidative aging of 2-hexanol. (b) Normalized peak area as a function of the aging time of various products of the thermo-oxidative aging of 2-hexanol.

concentration of 2-hexanol decreases by $\sim 42\%$ to a value of $c = 5.06 \text{ mg mL}^{-1}$. The concentration of 2-hexanone increases continuously from 48 h to 192 h up to a value of $c = 3.50 \text{ mg mL}^{-1}$. The resulting acetic acid also increases from 96 h to 192 h up to a value of $c = 0.101 \text{ mg m}^{-1}$ (*cf.* Fig. 8a). The two esters 2-hexyl formate and 2-hexyl acetate also increase from 96 h and from 120 h to 192 h, respectively (*cf.* Fig. 8b).

The results show that the iso-alcohol 2-hexanol is more stable against thermo-oxidative aging than the *n*-alcohols 1-hexanol or 1-octanol. After 192 h of aging, the initial concentration of 2-hexanol only decreases by 42%, whereas that of 1-hexanol decreased by 65% and that of 1-octanol by almost 73%. This is partly due to the fact that fewer aging products (*cf.* Table 1) can be formed during the aging of 2-hexanol than during the aging of 1-hexanol and 1-octanol. This could be explained that the resulting ketone 2-hexanone cannot be further oxidized, but can only react by oxidative C-C bond cleavage into further products.

The results show that the iso-alcohol 2-hexanol is more stable than the two *n*-alcohols. Furthermore, the shorter-chain *n*-alcohol 1-hexanol is more stable than the longer-chain 1-octanol. This is shown, among other things, by the fact that the initial concentration of 1-octanol decreases by ~73% and the initial concentration of 1-hexanol decreases by ~65% after 192 h aging time. This can also be explained by the fact that significantly more different products were formed during the aging of 1-octanol than during the aging of 1-hexanol. The initial concentration of 2-hexanol decreases by ~21% after 192 h of ageing time and significantly fewer different products were formed than during the aging of 1-hexanol and 1-octanol.

3.2.4. Fuel specific parameters of the aged alcohols. If the fuel-specific parameters such as the total acid number and the viscosity of the aged alcohols are considered, it can be seen that the total acid number (cf. Fig. 9a) for the *n*-alcohols 1-hexanol and 1-octanol rises strongly during aging, up to a maximum value of $TAN_{1\text{-hexanol}} = 67.61$ mg KOH per g and $TAN_{1\text{-octanol}} = 56.52$ mg KOH per g, respectively. This is due to the above-described formation of carboxylic acids during aging. The total acid number of 2-hexanol increases only slightly during aging to a maximum value of $TAN_{2\text{-hexanol}} = 2.41$ mg KOH per g, as significantly fewer carboxylic acids are formed during aging. The viscosity decreases during aging for all three alcohols (cf. Fig. 9b). It decreases by $\sim 34\%$ for 1-hexanol, by $\sim 28\%$ for 1-octanol and by $\sim 53\%$ for 2-hexanol. This is due to the formation

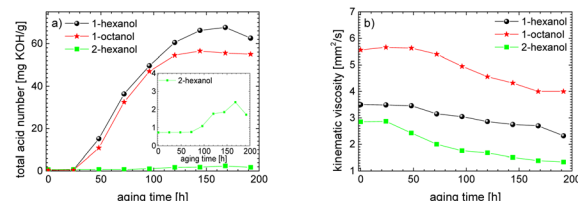


Fig. 9 (a) Total acid number as a function of the aging time of 1-hexanol (black spheres), 2-hexanol (green squares), and 1-octanol (red stars). (b) Kinematic viscosity as a function of the aging time of 1-hexanol (black spheres), 2-hexanol (green squares), and 1-octanol (red stars).

of aldehydes or ketones, acids, and esters, whose viscosity is lower due to the lower hydrogen bonding.

3.2.5. Carbon mass fraction of the liquid and the gas phase of thermo-oxidative aging. Since, among other things, the determination of the total acid number can neither determine exactly which acids are formed nor to what quantitative extent these are formed (the value of the total acid number can be falsified by the formation of esters), it is important to consider the composition in form of the carbon balance (Fig. 11).

As the experiment using the open aging setup (setup 1) does not allow determination of gaseous products and furthermore loss of volatile products occurred, the composition of the aged fuel has been further investigated in a closed system. While this allows to close the mass balance, air could not be used as an oxidant due to volume/pressure constraints. Therefore, the closed aging setup (setup 2, *cf.* Section 2.2.2) was used with a 30% aqueous hydrogen peroxide solution as oxidant. Aging with both setups (setup 1 and setup 2) shows similar aging effects and concentrations of the aging products. This can exemplarily be seen for the aging of 1-hexanol, 1-octanol, and 2-hexanol using setup 1 and setup 2 and the concentrations for the main products (*cf.* Fig. 10a-d). The concentration of 1-hexanol and 2-hexanol are slightly higher when aged in setup 2 than aged in setup 1. This can be due to the fact that the vapor pressure of the alcohols is significantly higher at higher temperatures. As a result, the alcohols can partially evaporate during aging in setup 1 when taking samples. If less alcohol is present, it can be less esterified and more acids remain in the fuel.

In order to further investigate the stability of the alcohols against thermo-oxidative aging and to determine the exact percentage carbon mass fraction of the resulting products in

the liquid and gas phase, the alcohols were aged for 120 h using setup 2 and the carbon mass balancing was carried out (see Section 2.3.5). Fig. 11 a shows the carbon mass fraction for the aging of the C₆-*n*-alcohol 1-hexanol; the corresponding percentage values are tabulated in the ESI in Table S1.† After 120 h of aging, 63.21 m% of the original 1-hexanol is still present. Furthermore, 0.86 m% hexanal and 6.25 m% hexanoic acid are present. In addition, 13.93 m% hexyl hexanoate was formed. The sum of the other resulting formed esters is 1.74 m%. Moreover, 3.10 m% CO₂ (due to oxidative decarboxylation), 0.917 m% 1-pentanol and 1.73 m% pentanoic acid are formed during aging. The remaining 8.26 m% are unbalanced products, *e.g.*, hexyl pentanoate, pentanal, 1-butanol or other products in the gas phase (*cf.* Tables 1 and S1 (ESI†)).

The aging of the C₈-*n*-alcohol 1-octanol (*cf.* Fig. 11b and Table S1 (ESI†)) shows, that 56.92 m% of 1-octanol is still present after 120 h of aging. In addition, 0.556 m% octanal and 6.99 m% octanoic acid are formed after 120 h. Furthermore, 16.32 m% octyl octanoate, in total 0.287 m% *n*-alcohols and in total 1.03 m% shorter-chain acids are formed during an aging time of 120 h. In addition, 3.83 m% additional esters are formed. Since 3.34 m% CO₂ is formed after 120 h, decarboxylation is indicated. The remaining 11.00 m% of unbalanced products are, for example, octyl propanoate, octyl pentanoate, octyl hexanoate, octyl heptanoate, heptanal, 1-butanol, pentanal or other products in the gas phase (*cf.* Tables 1 and S1 (ESI†)).

The carbon mass balance of the C₆-iso-alcohol 2-hexanol is shown in Fig. 11c and tabulated in Table S1 (ESI†). After 120 h of aging, 80.33 m% of 2-hexanol is still present. Furthermore, 10.09 m% of 2-hexanone is formed after 120 h of aging. Acetic acid is also formed with 0.032 m%. The formation of 1.40 m% carbon dioxide after 120 h of aging indicates decarboxylation. A

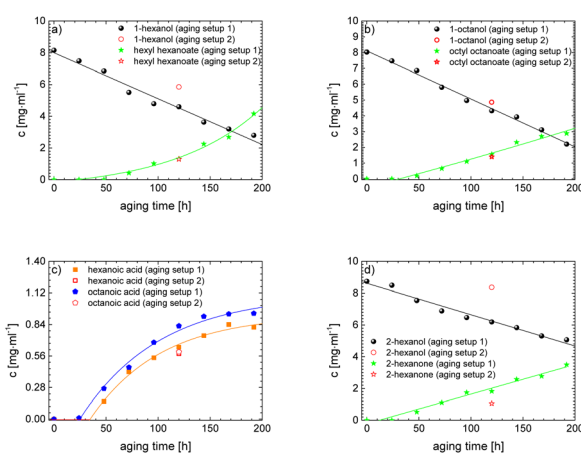


Fig. 10 (a) Concentration as a function of the aging time for 1-hexanol and hexyl hexanoate, aged with setup 1 (filled symbols) and aged with setup 2 (blank symbols). (b) Concentration as a function of the aging time of 1-octanol and octyl octanoate, aged with setup 1 (filled symbols) and aged with setup 2 (blank symbols). (c) Concentration as a function of the aging time of hexanoic acid and octanoic acid, aged with setup 1 (filled symbols) and aged with setup 2 (blank symbols). (d) Concentration as a function of the aging time of 2-hexanol and 2-hexanone, aged with setup 1 (filled symbols) and aged with setup 2 (blank symbols).

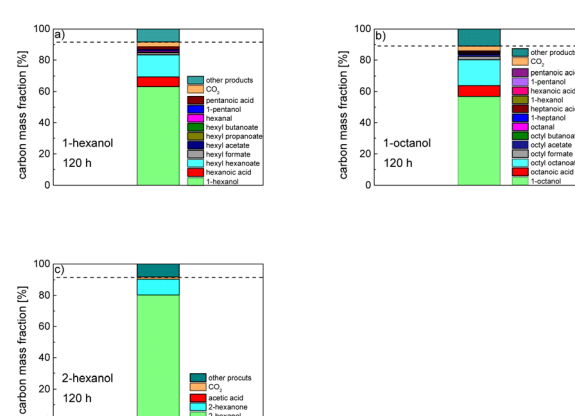


Fig. 11 (a) Carbon mass fraction of the thermo-oxidative aging (120 h) of 1-hexanol. Other products, which were not individually quantified, include hexyl pentanoate, pentanal, 1-butanol or other products in the gas phase. (b) Carbon mass fraction of the thermo-oxidative aging (120 h) of 1-octanol. Other products, which were not individually quantified, include octyl propanoate, octyl pentanoate, octyl hexanoate, octyl heptanoate, heptanal, 1-butanol, pentanal or other products in the gas phase. (c) Carbon mass fraction of the thermo-oxidative aging (120 h) of 2-hexanol. Other products, which were not individually quantified, include 2-hexyl formate, 2-hexyl acetate, 1-butanol or other products in the gas phase.



further 8.15 m% of unbalanced products can be, for example, 2-hexyl formate, 2-hexyl acetate, 1-butanol or other products in the gas phase (cf. Tables 1 and S1 (ESI[†])).

It follows from the results that iso-alcohols are more stable to thermo-oxidative aging than *n*-alcohols. One explanation for this is that an iso-alcohol can only be oxidized to a ketone and not further be oxidized to a carboxylic acid due to the non-terminal position of its hydroxy group. Another reason could be the inductive stabilization of the middle C-atoms, which reduces their reactivity. The terminal position of the hydroxy group of an *n*-alcohol enables direct oxidation to an aldehyde and further to a carboxylic acid. Since direct oxidation to acids is not possible with an iso-alcohol, the formation of an acid initially involves an oxidative C–C bond cleavage, which is significantly less likely than direct oxidation due to the high binding energy of the C–C bonds. Due to this fact, fewer esters are formed when aging an iso-alcohol, as the resulting acids are required for this. The results also show, that the chain length has an influence on thermo-oxidative aging. Due to oxidative C–C bond cleavage, more different acids and *n*-alcohols can be formed because the additional two carbon atoms mean there are more sites for the C–C bond to break. Due to the larger number of carboxylic acids and *n*-alcohols, a larger number of esters can also be formed through esterification.

4. Conclusion and outlook

This investigation is an important contribution for the widespread implementation of sustainable e-fuels. In this paper, the aging pathways of three promising alcohols, the two *n*-alcohols 1-hexanol and 1-octanol as well as the iso-alcohol 2-hexanol, were examined in detail depending on the aging time. This makes it possible to investigate the stability of alcohols depending on their chain length and their hydroxy group position. The focus here is on both the liquid phase of the fuel and the gas phase. The studies show that iso-alcohols are more stable against thermo-oxidative aging than *n*-alcohols. We observed, among other things, that significantly more aging products are formed when aging *n*-alcohols than when aging iso-alcohols. A large number of aldehydes, acids, shorter-chain *n*-alcohols and esters are formed when aging *n*-alcohols due to oxidation, decarboxylation, oxidative C–C bond cleavage and esterification. When aging iso-alcohol, significantly fewer decomposition products are formed through oxidation, decarboxylation, oxidative C–C bond cleavage and esterification. The investigation of important fuel-specific parameters such as the total acid number (TAN) and the kinematic viscosity shows that the total acid number of *n*-alcohols reaches values of up to $TAN_{n\text{-alcohol}} \sim 67.6$ mg KOH per g, while for iso-alcohol it only reaches values of up to $TAN_{\text{iso-alcohol}} \sim 2.4$ mg KOH per g. The kinematic viscosity values decrease during aging for both the *n*-alcohols and the iso-alcohol.

The carbon mass balance of the alcohols provides information about the exact composition of the aging products. For the two *n*-alcohols, ~63 m% for 1-hexanol and ~57 m% of 1-octanol are still present after an aging time of 120 h, while for 2-hexanol ~80 m% is still present. In addition, significantly fewer acids are formed with iso-alcohol (for iso-alcohol ~0.03%, for *n*-alcohols a total of ~8 m% or 7 m%). When examining the influence of the

chain length of the *n*-alcohols on aging, it is shown that the shorter-chain C₆-alcohol is more stable (~6 m% more still present after 120 h) than the longer-chain C₈-alcohol. This is probably due to the fact that the longer chain *n*-alcohol can form a greater variety of products.

It follows from the results of the time-dependent aging of the alcohols and the carbon mass balance for stability against thermo-oxidative aging:

$$\begin{aligned} \text{Stability}_{\text{longchain-}n\text{-alcohol}} &< \text{Stability}_{\text{shorterchain-}n\text{-alcohol}} \\ &< \text{Stability}_{\text{iso-alcohol}}. \end{aligned}$$

Since the stability of iso-alcohols is significantly higher than that of *n*-alcohols, consideration should be given using iso-alcohols as renewable fuels or fuel admixtures rather than *n*-alcohols. However, this only applies from the chemical standpoint of aging. To make a selection, further investigations into the combustion behaviour of *n*- or iso-alcohols as pure fuels or fuel mixtures are necessary. It is also useful to add an antioxidant to prevent or slow down aging and its effects.

Author contributions

Anne Lichtinger: conceptualization, investigation, validation, data acquisition, writing original draft, analysis and interpretation of data, approval of the version of the manuscript to be published. Maximilian J. Poller: conceptualization, analysis and interpretation of data, revising manuscript critically for important intellectual content, approval of the version of the manuscript to be published. Olaf Schröder: revising manuscript critically for important intellectual content, approval of the version of the manuscript to be published. Julian Türck: revising the manuscript critically for important intellectual content, approval of the version of the manuscript to be published. Thomas Garbe: revising manuscript critically for important intellectual content, approval of the version of the manuscript to be published. Jürgen Krahl: revising the manuscript critically for important intellectual content, approval of the version of the manuscript to be published. Markus Jakob: project administration, revising the manuscript critically for important intellectual content, approval of the version of the manuscript to be published. Jakob Albert: project administration, revising the manuscript critically for important intellectual content, approval of the version of the manuscript to be published.

Conflicts of interest

There are no conflicts to declare.

Acknowledgements

We thank the Forschungsvereinigung Verbrennungskraftmaschinen e.V. (FVV 601342) and the Oberfrankenstiftung (FP00067) for the financial support of the research. Additionally, we thank Michael Gröger and Dr Bernd Becker.



References

1 R. Pütz, European Policy On Future Road Mobility - Technology Neutrality Right Of Way Or Headed In The Wrong Direction?, *MVM*, 2022, **48**, 1–18.

2 Z. Allam, S. E. Bibri and S. A. Sharpe, The Rising Impacts of the COVID-19 Pandemic and the Russia–Ukraine War: Energy Transition, Climate Justice, Global Inequality, and Supply Chain Disruption, *Resources*, 2022, **11**, 99.

3 A. Lichtinger, M. J. Poller, J. Türck, O. Schröder, T. Garbe, J. Krahl, A. Singer, M. Jakob and J. Albert, Nile Red as a Fluorescence Marker and Antioxidant for Regenerative Fuels, *Energy Technol.*, 2023, **11**(11), 2300260.

4 P. Runge, C. Sölich, J. Albert, P. Wasserscheid, G. Zöttl and V. Grimm, Economic comparison of different electric fuels for energy scenarios in 2035, *Appl. Energy*, 2019, **233–234**, 1078–1093.

5 S. Schemme, R. C. Samsun, R. Peters and D. Stolten, Power-to-fuel as a key to sustainable transport systems – An analysis of diesel fuels produced from CO₂ and renewable electricity, *Fuel*, 2017, **205**, 198–221.

6 P. Runge, C. Sölich, J. Albert, P. Wasserscheid, G. Zöttl and V. Grimm, Economic comparison of electric fuels for heavy duty mobility produced at excellent global sites - A 2035 Scenario, *Appl. Energy*, 2023, **347**, 12137.

7 V. R. Surisetty, A. K. Dalai and J. Kozinski, Alcohols as alternative fuels: An overviewGeneral, *Appl. Catal., A*, 2011, **404**(1–2), 1–11.

8 V. Mahdavi and M. H. Peyrovi, Synthesis of C1–C6 alcohols over copper/cobalt catalysts, *Catal. Commun.*, 2006, **7**, 542–549.

9 S. Schemme, J. L. Breuer, R. C. Samsun, R. Peters and D. Stolten, Promising catalytic synthesis pathways towards higher alcohols as suitable transport fuels based on H₂ and CO₂, *J. CO₂ Util.*, 2018, **27**, 223–237.

10 R. Mayank, A. Ranjan and V. S. Moholkar, Mathematical models of ABE fermentation: review and analysis, *Crit. Rev. Biotechnol.*, 2013, **33**, 419–447.

11 M. Sherbi, M. Stuckart and J. Albert, Selective catalytic hydrogenation of biomass derived furans to secondary alcohols using Pt/polyoxometalate catalysts under mild reaction conditions, *Biofuels, Bioprod. Biorefin.*, 2021, **15**, 1431–1446.

12 M. Sherbi and J. Albert, Modeling and optimization of bio-2-hexanol production from biomass derived dimethylfuran using Pt/K3PW12O40 by response surface methodology, *Comput. Chem. Eng.*, 2021, **155**, 107546.

13 M. Jakob, *Optical Investigation of Diesel-Engine Related Combustion Processes*, 2015, DOI: [10.13140/RG.2.1.1912.2002](https://doi.org/10.13140/RG.2.1.1912.2002).

14 M. Nour, Z. Sun, A. I. El-Seesy and X. Li, Experimental evaluation of the performance and emissions of a direct-injection compression-ignition engine fueled with n-hexanol–diesel blends, *Fuel*, 2021, **302**, 121144.

15 A. García, J. Monsalve-Serrano, D. Villalta, M. Zubel and S. Pischinger, Potential of 1-octanol and di-n-butyl ether (DNBE) to improve the performance and reduce the emissions of a direct injected compression ignition diesel engine, *Energy Convers. Manage.*, 2018, **177**, 563–571.

16 F. Pradelle, S. L. Braga, A. R. F. A. Martins, F. Turkovics and R. N. C. Pradelle, Gum Formation in Gasoline and Its Blends: A Review, *Energy Fuels*, 2015, **29**, 7753–7770.

17 R. PEREIRA and V. PASA, Effect of mono-olefins and diolefins on the stability of automotive gasoline, *Fuel*, 2006, **85**, 1860–1865.

18 B. D. Batts and Z. Fathoni, A Literature Review on Fuel Stability Studies with Particular Emphasis on Diesel Oil, *Energy Fuels*, 1991, 2–21.

19 Y. K. Sharma, The Instability of Storage of Middle Distillate Fuels: A Review, *Pet. Sci. Technol.*, 2012, **30**, 1839–1850.

20 I. M. Rizwanul Fattah, H. H. Masjuki, M. A. Kalam, M. A. Hazrat, B. M. Masum, S. Imtenan and A. M. Ashraful, Effect of antioxidants on oxidation stability of biodiesel derived from vegetable and animal based feedstocks, *Renewable Sustainable Energy Rev.*, 2014, **30**, 356–370.

21 I. M. Rizwanul Fattah, H. H. Masjuki, M. A. Kalam, M. Mofijur and M. J. Abedin, Effect of antioxidant on the performance and emission characteristics of a diesel engine fueled with palm biodiesel blends, *Energy Convers. Manage.*, 2014, **79**, 265–272.

22 L. Botella, F. Bimbela, L. Martín, J. Arauzo and J. L. Sánchez, Oxidation stability of biodiesel fuels and blends using the Rancimat and PetroOXY methods. Effect of 4-allyl-2,6-dimethoxyphenol and catechol as biodiesel additives on oxidation stability, *Front. Chem.*, 2014, **2**, 43.

23 B. Schmidt and J. Hermanns, *Grundlagen der Organischen Chemie*, DeGruyter, Berlin, Boston, 2022.

24 S. Flitsch, P. M. Neu, S. Schober, N. Kienzl, J. Ullmann and M. Mittelbach, Quantitation of Aging Products Formed in Biodiesel during the Rancimat Accelerated Oxidation Test, *Energy Fuels*, 2014, **28**, 5849–5856.

25 T. Ogawa, S. Kajiya, S. Kosaka, I. Tajima and M. Yamamoto, Analysis of Oxidative Deterioration of Biodiesel Fuel, *SAE Int. J. Fuels Lubr.*, 2009, 1571–1583.

26 H. L. Fang and R. L. McCormick, Spectroscopic Study of Biodiesel Degradation Pathways, *SAE Technical Paper Series*, 2006.

27 B. Terry, R. L. McCormick and M. Natarajan, Impact of Biodiesel Blends on Fuel System Component Durability, *SAE Technical Paper Series*, 2006.

28 D. Prabhu and C. Rana, A Kinetic Approach To The Oxidation Of 1-Hexanol And Cyclohexanol Using Inorganic Oxidants, *Rasayan J. Chem.*, 2016, 139–143.

29 J. E. Gallot, M. P. Kapoor and S. Kaliaguine, Kinetics of 2-hexanol and 3-hexanol oxidation reaction over TS-1 catalysts, *AICHE J.*, 1998, **44**, 1438–1454.

30 T. Ishida, Y. Ogihara, H. Ohashi, T. Akita, T. Honma, H. Oji and M. Haruta, Base-free direct oxidation of 1-octanol to octanoic acid and its octyl ester over supported gold catalysts, *ChemSusChem*, 2012, **5**, 2243–2248.

31 A. H. Hussein, A. Khalil, M. Jahjah, M. Srour, R. Jahjah, N. Duget, M. Lemaire and D. Naoufal, Catalytic Properties



of Various Oxides and Mesoporous Materials Containing Niobium and Sulfate Ions, in the Oxidation Reaction of 1-Octanol, *Int. J. Org. Chem.*, 2018, **08**, 41–53.

32 Y. Kotolevich, E. Kolobova, E. Khramov, M. H. Farías, Y. Zubavichus, H. Tiznado, S. Martínez-González, V. Cortés Corberán, J. D. Mota-Morales, A. Pestryakov and N. Bogdanchikova, n-Octanol oxidation on Au/TiO₂ catalysts promoted with La and Ce oxides, *Mol. Catal.*, 2017, **427**, 1–10.

33 W. A. Mosher and D. M. Preiss, *The Mechanism of Aldehyde and Primary Alcohol Oxidation*, 1953, 5605–5607.

34 G. Jenzer, M. S. Schneider, R. Wandeler, T. Mallat and A. Baiker, Palladium-Catalyzed Oxidation of Octyl Alcohols in “Supercritical” Carbon Dioxide, *J. Catal.*, 2001, **199**, 141–148.

35 T. Iwahama, Y. Yoshino, T. Keitoku, S. Sakaguchi and Y. Ishii, Efficient oxidation of alcohols to carbonyl compounds with molecular oxygen catalyzed by N-hydroxyphthalimide combined with a Co species, *J. Org. Chem.*, 2000, **65**, 6502–6507.

36 C. Guillard, P. Theron, P. Pichat and C. Petrier, Evaluation of 1-octanol degradation by photocatalysis and ultrasound using SPME, *Water Res.*, 2002, 4263–4272.

37 Q. Li and F. Li, Recent advances in molecular oxygen activation via photocatalysis and its application in oxidation reactions, *Chem. Eng. J.*, 2021, **421**, 129915.

38 H. W. Gardner, Oxygen Radical Chemistry of Polyunsaturated Fatty Acids, *Free Radical Biol. Med.*, 1988, **1989**, 65–86.

39 R. A. Sheldon and J. K. Kochi, Metal-Catalyzed Oxidations of Organic Compounds, *Mechanistic Principles and Synthetic Methodology Including Biochemical Processes*, Elsevier Science, New York, London, Toronto, Sydney, San Francisco, 1981.

40 D. R. Larkin, The Role of Catalysts in the Air Oxidation of Aliphatic Aldehydes, *J. Org. Chem.*, 1990, 1563–1568.

41 J. Buddrus and B. Schmidt, *Grundlagen der Organischen Chemie*, DeGruyter, Berlin, München, Boston, 5th edn, 2014.

42 X. Zhao, T. Zhang, Y. Zhou and D. Liu, Preparation of peracetic acid from hydrogen peroxide, *J. Mol. Catal. A: Chem.*, 2007, **271**, 246–252.

